Available online at: https://ijact.in

Date of Submission	28/06/2019
Date of Acceptance	10/08/2019
Date of Publication	31/08/2019
Page numbers	3324-3335(12 Pages)

Cite This Paper: Pankaj Sahu, MK Verma. Online monitoring of voltage stability margin and its control through STATCOM, 8(8), COMPUSOFT, An International Journal of Advanced Computer Technology. PP. 3324-3335.

ISSN:2320-0790

compusoft
An International Journal of Advanced Computer Technology

ONLINE MONITORING OF VOLTAGE STABILITY MARGIN AND ITS CONTROL THROUGH STATCOM

Pankaj Sahu[1], M. K. Verma[2]

[1]Department of Electrical Engineering, IIT (BHU), Varanasi, India
[2]Department of Electrical Engineering, IIT (BHU), Varanasi, India

Abstract: Voltage instability has been of serious concern for researchers and utilities since last few decades as several incidences of system blackout initiated by voltage instability have been observed in different parts of the world. With advent of synchrophasor technology, it seems possible to monitor and control voltage stability of the system in real time framework. This paper proposes online monitoring of voltage stability margin based on optimally placed phasor measurement units (PMUs), and its control through Static Synchronous Compensator (STATCOM). STATCOM has been placed at the critical bus obtained based on minimum real and reactive power loadability for majority of line outages. STATCOM injects reactive power to the bus based on deviation of bus voltage from its reference value. Bus voltages are determined at regular intervals using measurements obtained by PMUs, and reactive power is injected to the bus online, accordingly. Enhanced voltage stability margin as a result of reactive power injection by STATCOM is monitored at regular interval. Effectiveness of proposed approach of online monitoring and control of voltage stability margin has been validated based on simulations carried out on IEEE 14-bus system, New England 39- bus system and a practical Indian system representing power network of nine states and union territories of Indian system.

Keywords:voltage stability; nose curves; static synchronous compensator (STATCOM); phasor measurement unit (PMU)

I. INTRODUCTION

Maintenance of voltage stability is an important aspect for secure operation of power systems. Voltage instability may result in appearance of unacceptable low voltages in a significant part of network leading to voltage collapse in a large area [1]. Several control measures have been suggested to protect the system against voltage collapse. One major cause of voltage instability is lack of reactive support. Transmission of reactive power is difficult particularly under stressed conditions. Therefore, local reactive support at critical buses seems a viable solution against voltage instability. Advancement in power electronics technology has led to development of Flexible AC Transmission System (FACTS) controllers that can effectively control voltage stability of the system [2]. Static Synchronous Compensator (STATCOM) belonging to FACTS family is a shunt controller capable to enhance voltage stability margin by injecting reactive power to the bus. Considering high cost, it is important to install STATCOM at optimal location. Generally, sufficient reactive power support at the critical bus or weakest bus of the system improves voltage stability margin. The *L*-index based method to determine critical buses for the placement of STATCOM has been considered [3-4]. The *P-V* and *Q-V* curves based technique have been widely used since the voltage collapse of Tokyo for optimal location and sizing of STATCOM [5-6]. These techniques are time consuming and expansive. Many heuristic approaches have been applied to find location and sizing of FACTS devices. Mixed integer linear and non-linear programming has been used to find optimal size and location of FACTS devices. However, difficulty arises due to local minima and computational efforts [7]. Particle Swarm Optimization (PSO) is an evolutionary computation technique that can be used to solve STATCOM size and allocation problem. This technique has been applied in advancing many issues of power system such as economic load dispatch [8], generation expanses [9] and short term load forecasting [10]. Particle Swarm Optimization based technique for optimal location and size of STATCOM to improve loadability and voltage stability is reported [11]. Bangjun Lei and ShuminFei proposed an Innovative Nonlinear (IN) H_∞control for STATCOM to improve voltage stability of power system network [12]. In this work, Hamiltonian function method has been used to design the IN H_∞control for STATCOM. A systematic method for short-term voltage stability improvement has been proposed that determines critical buses using concept of trajectory sensitivity [13]. Direct power control by STATCOM based on transit of active power as a result of injection/absorption of reactive power has been proposed [14].

Most of the research has considered studies on role of STATCOM in voltage stability enhancement of offline systems. With advent of Phasor Measurement Units (PMUs), it seems possible to monitor and control voltage stability of online systems [15]. This paper proposes monitoring and control of voltage stability of online systems employed with STATCOM using Phasor Measurement Units. Considering STATCOM placement to be an offline strategy, it has been optimally placed in the system based on critical bus obtained by Continuation Power Flow (CPF) method [16]. However, monitoring and control of voltage stability margin as a result of reactive power injection by STATCOM to the critical bus has been proposed for the online systems using bus voltages measured by phasor measurement units at regular intervals.

II. STATCOM PLACEMENT STRATEGY

As STATCOM placement is an offline strategy its optimal location is decided based on maximum loadability obtained by continuation power flow (CPF) method. Continuation power flow is run for the system intact case and all the single line outage cases to determine maximum real power as well as maximum reactive power loadability of each bus. Maximum real power loadability and maximum reactive power loadability have been obtained by varying real power and reactive power demand as per following:

$$P_{D_i} = P_{D_{ib}}(1+\lambda_{ip}) \quad (1)$$

$$Q_{D_i} = Q_{D_{ib}}(1+\lambda_{iq}) \quad (2)$$

where,

P_{D_i} = Real power demand at bus-*i*

Q_{D_i} = Reactive power demand at bus-*i*

$P_{D_{ib}}$ = Real power demand at bus-*i* at the base case operating point

$Q_{D_{ib}}$ = Reactive power demand at bus-*i* at the base case operating point

λ_{ip} = Fraction of real power demand increase at bus-*i*

λ_{iq} = Fraction of reactive power demand increase at bus-*i*

STATCOM is placed at the bus having lowest real power loadability as well as reactive power loadability for majority of contingency cases.

In this work, voltage regulator model of STATCOM (shown in figure-1) has been considered that injects reactive power to the bus based on bus voltage magnitude differing from its reference value, subject to maximum and minimum limit of current injection (viz. $i_{max}$and i_{min} as shown).

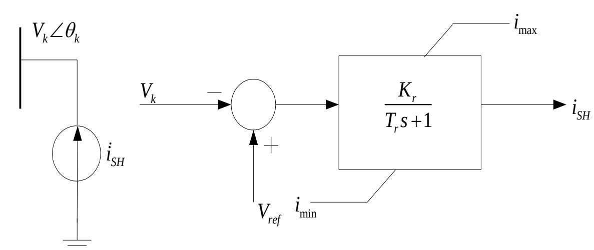

$V_k\angle\theta_k$ = node voltage and angle

Figure 1: STATCOM model

State equation pertaining to dynamic model of STATCOM is given by,

$$\dot{i}_{SH} = (K_r(V_{ref} - V_k) - i_{SH})/T_r \quad (3)$$

where, i_{SH} = Current injected to bus by STATCOM

V_{ref} = Reference value of bus voltage magnitude

V_k = Voltage of bus-*k* (the bus where STATCOM is placed)

K_r = Gain of voltage regulator

T_r = Time constant of voltage regulator

Reactive power (Q_{SH}) injected by STATCOM is given by,

$$Q_{SH} = i_{SH}V \quad (4)$$

as bus voltage and injected current are considered to be in phase quadrature.

III. METHODOLOGY FOR ONLINE CONTROL OF VOLTAGE STABILITY MARGIN THROUGH STATCOM

Voltage stability margin of the system employed with Static Compensator (STATCOM) is monitored online using Phasor Measurements Unit (PMU) measurements and pseudo measurements performed at three operating points. As operating points keep on changing due to change in operating conditions/network topology, fresh PMU measurements are performed and updated voltage stability information is obtained at regular intervals. PMUs are optimally placed in the system based on results of binary integer linear programming [18] ensuring full network observability even in case of loss of few PMUs. Pseudo measurements are performed as per following network observability rules:

1. If voltage and current phasor at one end of a branch are known voltage phasor at the other end of the branch can be computed using Ohm's law.
2. If voltage phasors at both the ends of a branch are known, branch current can be calculated.
3. If there exists a zero-injection bus with all branch currents known except one, the unknown branch current can be calculated using Kirchhoff's current law (KCL)

PMU measurements and pseudo measurement are performed at three operating points to determine voltage magnitude of all the buses. Reactive power injection to the bus by STATCOM at the three operating points is computed as per (3) and (4). Voltage stability margin (maximum real power loadability as well as reactive power loadability) of the system employed with STATCOM is obtained by quadratic fitting of nose curves based on PMU measurements and pseudo measurements obtained at three operating points as per following:

Real power demand (P_{D_i}) versus voltage magnitude V_i curve (*P*-*V* curve) of bus-*i* (shown in figure-2)may be approximately obtained by solution of quadratic equation,

$$P_{D_i} = a_{1i}V_i^2 + a_{2i}V_i + a_{3i} \tag{5}$$

where, a_{1i} , a_{2i} and a_{3i} are constants

Differentiating P_{D_i} with respect to V_i ,

$$\frac{dP_{D_i}}{dV_i} = 2a_{1i}V_i + a_{2i} \tag{6}$$

At nose point of *P*-*V* curve, $\frac{dP_{D_i}}{dV_i}$ = 0. Therefore, from (6),

$$V_i^{np} = -\frac{a_{2i}}{2a_{1i}} \tag{7}$$

where, V_i^{np} = voltage magnitude of bus-*i* at the nose point of *P*-*V* curve (shown in figure-2).

From (5) and (7),

$$P_{D_i}^n = -\frac{a_{2i}^2}{4a_{1i}} + a_{3i} \tag{8}$$

where, $P_{D_i}^n$ = Real power demand of bus-*i* at the nose point of *P*-*V* curve (shown in figure-2).

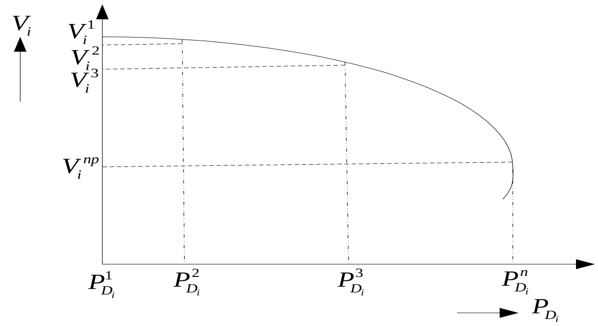

Figure 2: *P*-*V* curve of bus-*i*

Reactive power demand (Q_{D_i}) versus voltage magnitude (V_i) curve (*Q*-*V* curve) of bus-*i* (shown in figure-3) may be approximately obtained by solution of quadratic equation,

$$Q_{D_i} = b_{1i}V_i^2 + b_{2i}V_i + b_{3i} \tag{9}$$

where, b_{1i} , b_{2i} and b_{3i} are constants.

Differentiating Q_{D_i} with respect to V_i ,

$$\frac{dQ_{D_i}}{dV_i} = 2b_{1i}V_i + b_{2i} \tag{10}$$

At the nose point of *Q*-*V* curve, $\frac{dQ_{D_i}}{dV_i}$ = 0, Therefore, from (10),

$$V_i^{nq} = -\frac{b_{2i}}{2b_{1i}} \tag{11}$$

where, V_i^{nq} = voltage magnitude of bus-*i* at the nose point of *Q*-*V* curve (shown in figure-3).

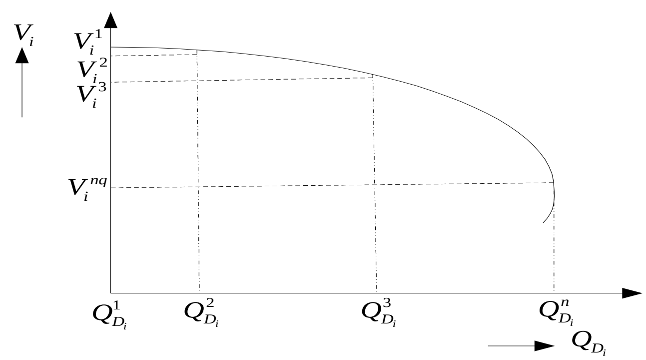

Figure 3: *Q*-*V* curve of bus-*i*

From (9) and (11),

$$Q_{D_i}^n = -\frac{b_{2i}^2}{4b_{1i}} + b_{3i} \tag{12}$$

where, $Q_{D_i}^n$ = Reactive power demand of bus-*i*at the nose point of *Q*-*V* curve (shown in figure-3).

Constants a_{1i}, a_{2i} and a_{3i} are obtained by solution of equations:

$$P_{D_i}^1 = a_{1i}(V_i^1)^2 + a_{2i}V_i^1 + a_{3i} \quad (13)$$

$$P_{D_i}^2 = a_{1i}(V_i^2)^2 + a_{2i}V_i^2 + a_{3i} \quad (14)$$

$$P_{D_i}^3 = a_{1i}(V_i^3)^2 + a_{2i}V_i^3 + a_{3i} \quad (15)$$

where, V_i^1, V_i^2, V_i^3 (shown in figure-2 and in figure-3) correspond to voltage magnitude of bus-*i* at operating points 1, 2 and 3, respectively, and $P_{D_i}^1$, $P_{D_i}^2$ and $P_{D_i}^3$ (shown in figure-2) correspond to real power demand of bus-*i* at operating points 1, 2 and 3, respectively.

Evaluated constants a_{1i}, a_{2i} and a_{3i} are used to find maximum real power loading of bus-*i* using (8).

Constants b_{1i}, b_{2i} and b_{3i} are obtained by solution of equations:

$$Q_{D_i}^1 = b_{1i}(V_i^1)^2 + b_{2i}V_i^1 + b_{3i} \quad (16)$$

$$Q_{D_i}^2 = b_{1i}(V_i^2)^2 + b_{2i}V_i^2 + b_{3i} \quad (17)$$

$$Q_{D_i}^3 = b_{1i}(V_i^3)^2 + b_{2i}V_i^3 + b_{3i} \quad (18)$$

where, $Q_{D_i}^1$, $Q_{D_i}^2$ and $Q_{D_i}^3$ (shown in figure-3) correspond to reactive power demand of bus-*i* at operating points 1, 2 and 3, respectively.

Evaluated constants b_{1i}, b_{2i} and b_{3i} are used to find maximum reactive power loadability of bus-*i* using (12).

Constants a_{1i}, a_{2i}, a_{3i}, b_{1i}, b_{2i} and b_{3i} for each of the load buses are evaluated using voltage magnitude, real power demand and reactive power demand obtained by PMU measurements/pseudo measurements performed at operating points 1, 2 and 3, respectively. Evaluated constants predict maximum real power loadability as well as maximum reactive power loadability of each bus using (8) and (12), respectively. Minimum out of maximum real power loadability of all the load buses present in the system is considered as maximum real power loadability of the system, and corresponding bus is considered as the most critical bus based on maximum real power loadability. Minimum out of maximum reactive power loadability of all the load buses present in the system is considered as maximum reactive power loadability of the system, and corresponding bus is considered as the most critical bus based on maximum reactive power loadability criterion. The flow chart for online monitoring of voltage stability margin and its control using STATCOM is shown in figure-4. Since, maximum loadability of a real time system keeps on changing with change in operating conditions; it is proposed to update maximum loadability as well as most critical bus information based on new PMU measurements obtained, at regular intervals. Flowchart shown in figure-4 assumes very high initial maximum loadability of 10,000 MW and 10,000 MVAR, respectively, keeping in mind such values to be higher than maximum loadability of any of the load buses present in the system, and keeps on reducing these till maximum real power as well as reactive power loadability of the most critical bus are obtained. After each PMU measurement, STATCOM injects reactive power as per (3) and (4).

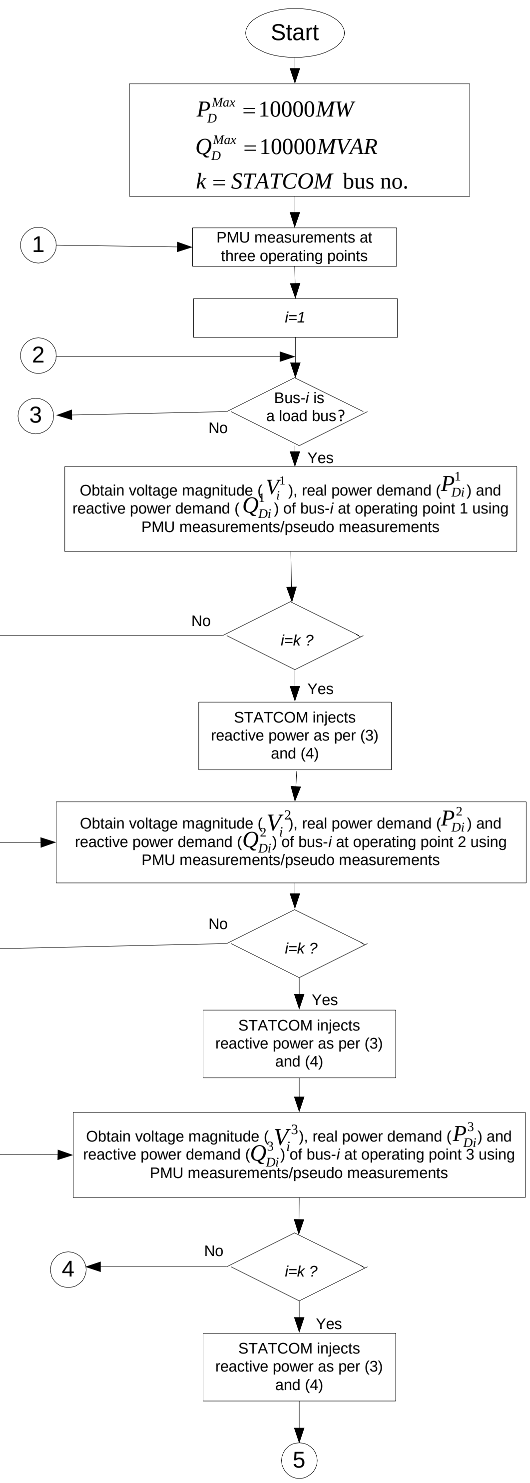

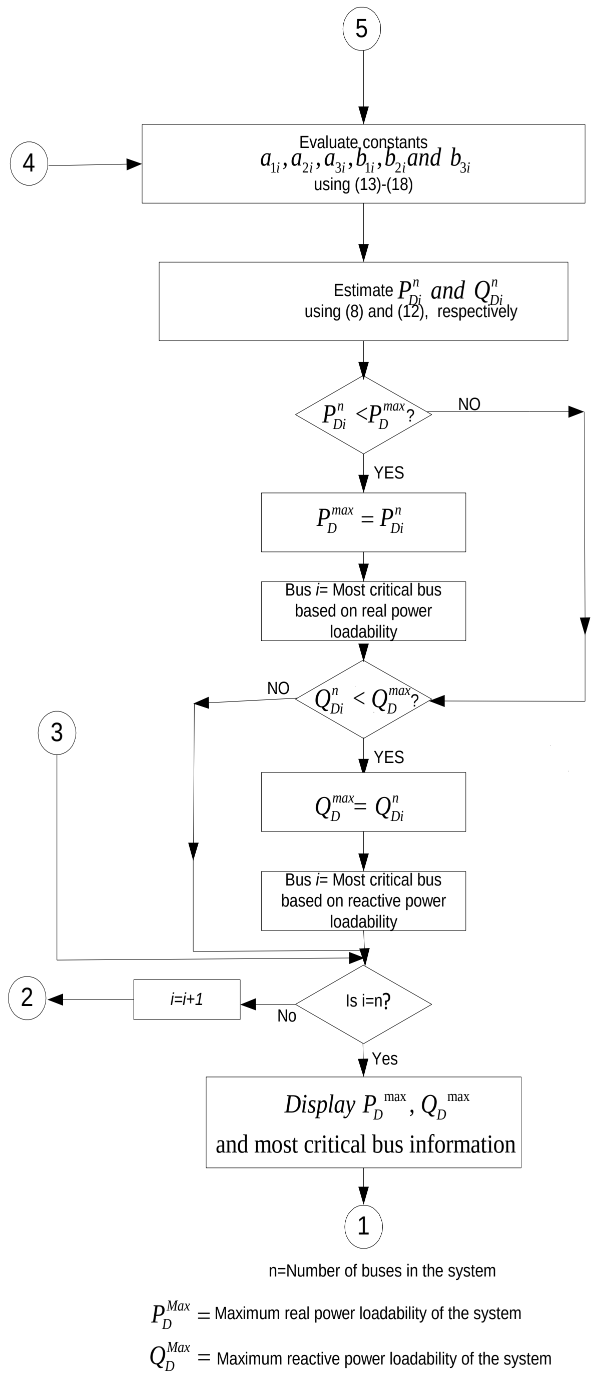

Figure 4: Flowchart for online control of maximum loadability using STATCOM

IV. RESULTS AND DISCUSSION

Case studies were performed on IEEE 14-bus system, New England 39-bus system, and a practical 246-bus Northern Region Power Grid (NRPG) system representing power network of seven states and two union territories of India.All simulations have been done in MATLAB linked PSAT software. We have used MATLAB 2013a and psat-2.1.9-mat. We have used MATLAB programming to find the voltage stability margin using generalized curve fitting technique utilizing three points. We have used PSAT software to obtain voltage stability margin by running continuation power flows. In PSAT software .mdl file has been constructed using the data given in references. In MATLAB .m file has been constructed.Simulation results obtained on three systems are presented below:

A. IEEE 14-Bus System [17]

IEEE 14-Bus System consists of two synchronous generators (at bus numbers 1 and 2), three synchronous condensers (at bus numbers 3, 6, 8), and 20 transmission lines (including three transformers). Single-line-diagram of the system is shown in figure-5.

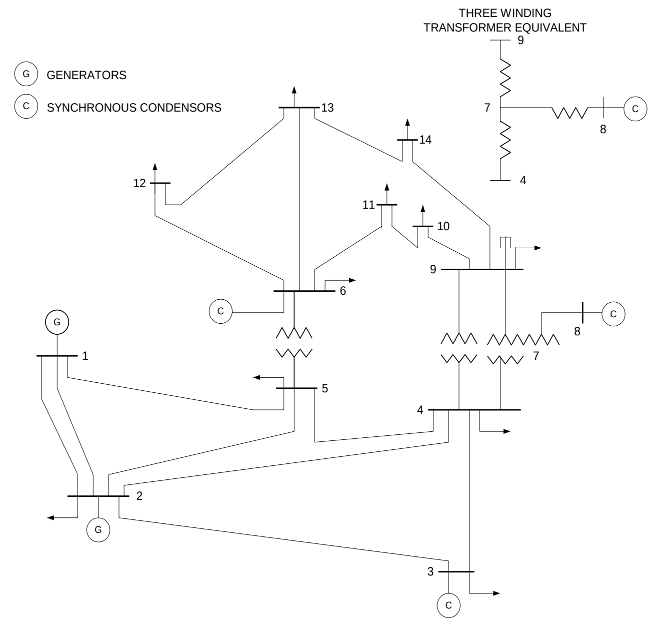

Figure 5: IEEE 14-Bus System

Continuation power flows were run to determine maximum real power loadability as well as maximum reactive power loadability of each bus for the system intact case and all the single line outage cases. For running continuation power flows, real and reactive power demand at each bus was varied as per (1) and (2), respectively. Maximum real power loadability (P_D^{Max}) along with critical bus number based on real power loadability, have been shown in Table I for the system intact case and few critical contingency cases. Maximum reactive power loadability (Q_D^{Max}) along with critical bus number based on reactive power loadability, have been shown in Table II for the system intact case and few critical contingency cases. It is observed from Table I and Table II that bus-5 is the most critical bus based on real power loadability as well as reactive power loadability for majority of critical contingencies. Therefore, bus-5 was selected as the optimal location for the placement of STATCOM.

TABLE I
MAXIMUM REAL POWER LOADABILITY OF CRITICAL BUS UNDER CRITICAL CONTINGENCIES OBTAINED BY CPF METHOD (IEEE 14-BUS SYSTEM)

S. No.	C.C.	P_D^{Max} (MW)	C.B.
1	Intact Case	40.20	5
2	1-2	16.49	5
3	2-3	30.11	4
4	2-4	32.91	5
5	1-5	34.50	5
6	2-5	35.26	5

C.C. = Critical Contingency, P_D^{Max} = Maximum Active Power Loadability, C.B. = Critical Bus

TABLE II
MAXIMUM REACTIVE POWER LOADABILITY OF CRITICAL BUS UNDER CRITICAL CONTINGENCIES OBTAINED BY CPF METHOD (IEEE 14-BUS SYSTEM)

S. No.	C.C.	Q_D^{Max} (MVAR)	C.B.
1	Intact Case	8.46	5
2	1-2	0.54	5
3	2-3	3.07	4
4	9-14	5.22	14
5	6-13	6.04	13
6	9-10	6.10	10

C.C. = Critical Contingency, Q_D^{Max} = Maximum Reactive Power Loadability, C.B. = Critical Bus

PMUs were placed at bus numbers 2, 4, 5, 6 and 9 based on results of binary integer linear programming [18] ensuring full network observability even in case of loss of few PMUs. Maximum real and reactive power loadability of the system with STATCOM placed at bus-5 were calculated for the system intact case and all the single line outage cases using flowchart shown in figure-4. In order to validate effectiveness of STATCOM placement strategy, real and reactive power loadability were also calculated for the system in the absence of STATCOM, based on flowchart presented in figure-4 ignoring blocks corresponding to STATCOM. Real and reactive power loadability were also calculated using continuation power flow (CPF) method for the system with and without STATCOM. Real and reactive power loadability of the system with and without STATCOM has been shown in Table III and IV respectively, for the system intact case and few critical contingency cases. It is observed from Table III and Table IV that placement of STATCOM at optimal location (viz. bus number 5) results in significant enhancement in voltage stability margin. Figure-6 shows a comparison of the nose curves of critical bus 5 obtained using proposed approach with and without STATCOM for the line outage 2-3 using real power. Figure-7 also shows a comparison of the nose curves of critical bus 5 obtained using proposed approach with and without STATCOM for the line outage 2-3 using reactive power. It is observed from figures-6 and 7 that STATCOM placed at bus-5 yields considerable enhancement in voltage stability margin.

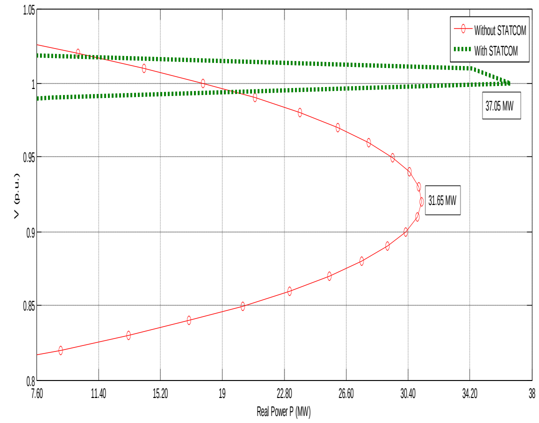

Figure 6: Comparison of *P-V* curves of critical bus 5 with STATCOM and without STATCOM for line outage 2-3 based on PMU measurements

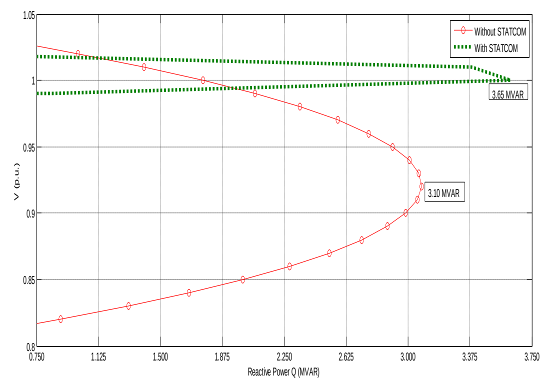

Figure 7: Comparison of *Q-V* curves of critical bus 5 with STATCOM and without STATCOM for line outage 2-3 based on PMU measurements

TABLE III
REALPOWERLOADABILITYOFTHESYSTEMWITHANDWITHOUT STATCOM

S. No.	Critical Contingency	PMU Measurements		CPF Method	
		Without STATCOM P_D^{Max} (MW)	With STATCOM at bus- 5 P_D^{Max} (MW)	Without STATCOM P_D^{Max} (MW)	With STATCOM at bus-5 P_D^{Max} (MW)
1	Intact	39.44	49.60	40.20	43.77
2	1-2	17.78	20.20	16.49	17.63
3	2-3	31.65	37.05	30.11	33.42
4	2-4	32.76	43.71	32.91	38.32
5	1-5	37.39	40.66	34.50	39.03
6	2-5	35.64	42.93	35.26	44.59

TABLE IV
REACTIVEPOWERLOADABILITYOFTHESYSTEMWITHANDWITHOUT STATCOM

S. No.	Critical Contingency	PMU Measurements		CPF Method	
		Without STATCOM Q_D^{Max} (MVAR)	With STATCOM at bus- 5 Q_D^{Max} (MVAR)	Without STATCOM Q_D^{Max} (MVAR)	With STATCOM at bus-5 Q_D^{Max} (MVAR)
1	Intact	7.81	9.25	8.46	9.05
2	1-2	0.56	1.27	0.54	0.58
3	2-3	3.10	3.65	3.07	4.73
4	6-13	5.57	9.08	6.04	6.38
5	9-14	4.68	7.31	5.22	6.44
6	9-10	5.64	8.30	6.10	6.50

B. New England 39-Bus System [19]

The New England 39-Bus System (shown in figure-8) has 10 generators and 46 transmission lines with 12 zero-injection buses at bus numbers 1, 2, 5, 6, 9, 10, 11, 13, 14, 17, 19 and 22 [19].

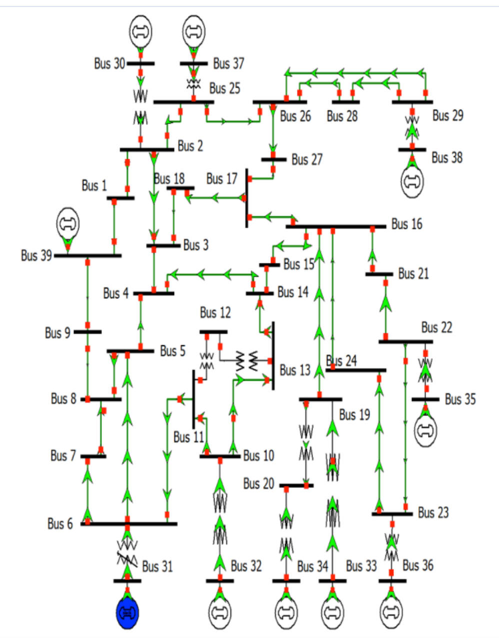

Figure 8: New England 39-Bus System

TABLE V
MAXIMUM REAL POWER LOADABILITY OF CRITICAL BUS UNDER CRITICAL CONTINGENCIES OBTAINED BY CPF METHOD (NEW ENGLAND 39-BUS SYSTEM)

S. No	C.C.	P_D^{Max} (MW)	C.B.
1	Intact Case	1686.83	29
2	21-22	930.60	23
3	28-29	989.42	29
4	22-35	1099.98	29
5	10-32	1102.82	29
6	29-38	2380	20

C.C. = Critical Contingency, P_D^{Max} = Maximum Active Power Loadability, C.B. = Critical Bus

TABLE VI
MAXIMUM REACTIVE POWER LOADABILITY OF CRITICAL BUS UNDER CRITICAL CONTINGENCIES OBTAINED BY CPF METHOD (NEW ENGLAND 39-BUS SYSTEM)

S. No.	C.C.	Q_D^{Max} (MVAR)	C.B.
1	Intact Case	151.01	29
2	2-25	51.26	25

3	29-38	72.10	20
4	28-29	88.58	29
5	10-32	98.73	29
6	15-16	168.90	15

C.C. = Critical Contingency, Q_D^{Max} = Maximum Reactive Power Loadability, C.B. = Critical Bus

21 PMUs were placed at bus numbers 4, 8, 12, 16, 18, 20, 23, 25, 26, 27, 29, 30, 31, 32, 33, 34, 35, 36, 37, 38 and 39 based on results of binary integer linear programming [18] ensuring full network observability even in case of loss of few PMUs. Maximum real and reactive power loadability of the system with STATCOM placed at bus number 29 were calculated for the system intact case and all the single line outage cases using flowchart shown in figure-4. In order to meet efficiency of STATCOM placement strategy, real and reactive power loadability were also calculated for the system in the absence of STATCOM, based on flowchart presented in figure-4 ignoring blocks corresponding to STATCOM. Real power and reactive power loadability were also calculated using continuation power flow (CPF) method for the system with and without STATCOM. Real and reactive power loadability of the system with and without STATCOM has been shown in Table VII and Table VIII respectively, for the system intact case and few critical contingency cases. It is observed from Table VII and VIII that placement of STATCOM at optimal location (viz. bus number 29) results in significant enhancement in voltage stability margin. Figure-9 shows a comparison of the nose curves of critical bus 29 obtained using proposed approach with and without STATCOM for the line outage 29-38. Figure-10 also shows a comparison of the nose curves of critical bus 29 obtained using proposed approach with and without STATCOM for the line outage 29-38. It is observed from figures-9 and 10 that STATCOM placed at bus-29 yields considerable enhancement in voltage stability margin.

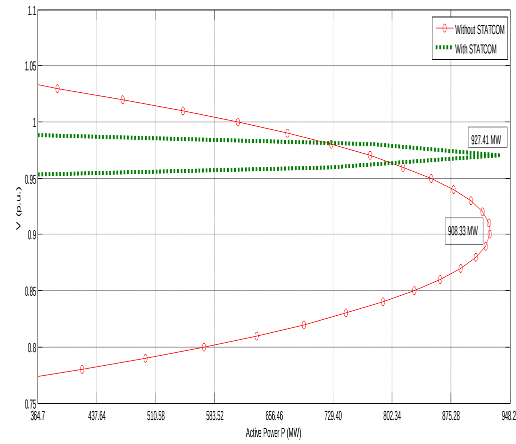

Figure 9: Comparison of *P-V* curves of critical bus 29 with STATCOM and without STATCOM for line outage 21-22 based on PMU measurements

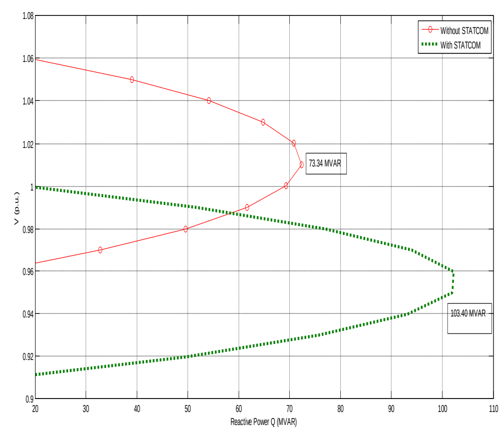

Figure 10: Comparison of *Q-V* curves of critical bus 29 with STATCOM and without STATCOM for line outage 29-38 based on PMU measurements

TABLE VII
REALPOWERLOADABILITYOFTHESYSTEMWITHANDWITHOUT STATCOM

S. No.	Critical Contingency	PMU Measurements Without STATCOM P_D^{Max} (MW)	PMU Measurements With STATCOM at bus-29 P_D^{Max} (MW)	CPF Method Without STATCOM P_D^{Max} (MW)	CPF Method With STATCOM at bus-29 P_D^{Max} (MW)
1	Intact	1363.64	1419.85	1686.83	1702.68
2	28-29	856.17	926.73	989.42	1003.23
3	21-22	908.33	927.41	930.60	943.28
4	22-35	1108.49	1117.63	1099.98	1104.45
5	10-32	1114.16	1144.15	1102.82	1107.47

TABLE VIII
REACTIVEPOWERLOADABILITYOFTHESYSTEMWITHANDWITHOUT STATCOM

S. No.	Critical Contingency	PMU Measurements Without STATCOM Q_D^{Max} (MVAR)	PMU Measurements With STATCOM at bus-29 Q_D^{Max} (MVAR)	CPF Method Without STATCOM Q_D^{Max} (MVAR)	CPF Method With STATCOM at bus-29 Q_D^{Max} (MVAR)
1	Intact	122.08	127.11	151.01	157.23
2	28-29	76.65	82.97	88.58	98.32
3	29-38	73.34	103.40	72.10	75.91
4	15-16	142.60	150.93	168.90	169.41

5	2-25	42.10	43.45	51.26	51.97
6	10-32	99.74	102.43	98.73	99.15

C. 246-Bus NRPG System [20]

The 246-bus Northern Regional Power Grid (NRPG) system represents power network of seven states (Jammu and Kashmir, Himachal Pradesh, Punjab, Haryana, Rajasthan, Uttarakhand and Uttar Pradesh) and two union territories (Delhi and Chandigarh) of India. The system consists of 42 generators, 36 transformers and 15 zero-injection buses at numbers 63, 75, 81, 102, 103, 104, 107, 122, 155, 180, 210, 226, 237, 241and 244. The single-line-diagram of the system is shown in figure-11.

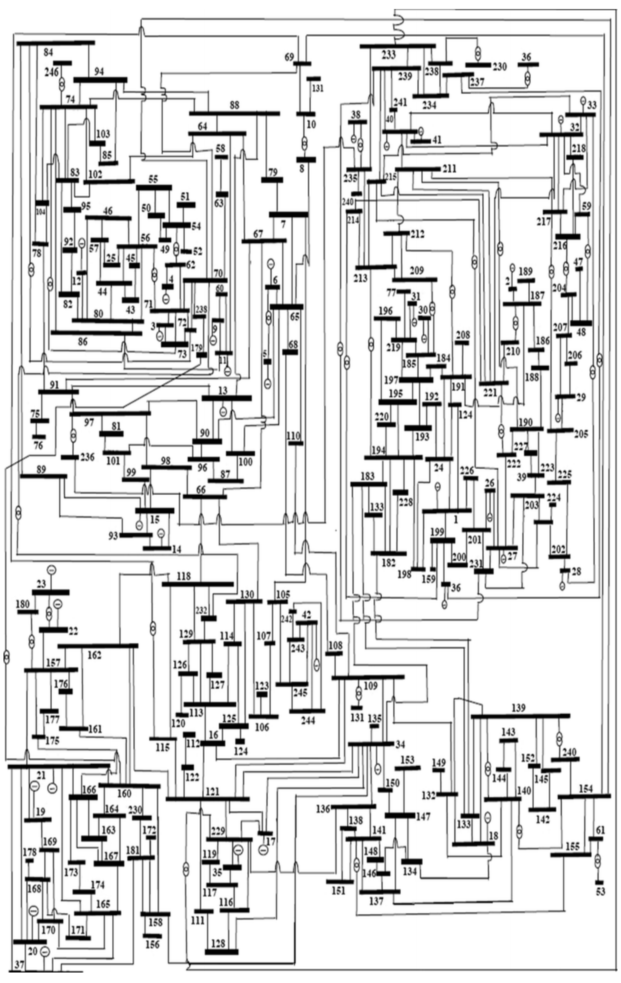

Figure 11: 246-bus NRPG system

Continuation power flows were run to determine maximum real power loadability as well as maximum reactive power loadability of each bus for the system intact case and all the single line outage cases. For running continuation power flows, real and reactive power demand at each bus was varied as per (1) and (2), respectively. Maximum real power loadability (P_D^{Max}) along with critical bus number based on real power loadability, have been shown in Table IX for the system intact case and few critical contingency cases. Maximum reactive power loadability (Q_D^{Max}) along with critical bus number based on reactive power loadability, have been shown in Table X for the system intact case and few critical contingency cases. It is observed from Table IX and Table X that bus-174 is the most critical bus based on real power loadability as well as reactive power loadability for majority of critical contingencies. Therefore, bus-174 was selected as the optimal location for the placement of STATCOM.

TABLE IX
MAXIMUM REAL POWER LOADABILITY OF CRITICAL BUS UNDER CRITICAL CONTINGENCIES OBTAINED BY CPF METHOD (NRPG 246-BUS SYSTEM)

S. No.	C.C.	P_D^{Max} (MW)	C.B.
1	Intact Case	641.84	174
2	173-174	344.69	174
3	40-41	383.75	174
4	166-173	434.69	174
5	156-158	476.93	158
6	194-198	518.86	174

C.C. = Critical Contingency, P_D^{Max} = Maximum Active Power Loadability, C.B. = Critical Bus

TABLE X
MAXIMUM REACTIVE POWER LOADABILITY OF CRITICAL BUS UNDER CRITICAL CONTINGENCIES OBTAINED BY CPF METHOD (NRPG 246-BUS SYSTEM)

S. No.	C.C.	Q_D^{Max} (MVAR)	C.B.
1	Intact Case	51.11	174
2	63-70	19.33	156
3	173-174	27.45	174
4	40-41	30.56	174
5	156-158	34.07	158
6	166-173	34.61	174

C.C. = Critical Contingency, Q_D^{Max} = Maximum Reactive Power Loadability, C.B. = Critical Bus

97 PMUs were placed at bus numbers 6, 7, 8, 10, 14, 18, 21, 22, 23, 24, 32, 33, 34, 40, 42, 45, 48, 54, 55, 57, 60, 61, 62, 65, 68, 70, 73, 74, 75, 78, 79, 80, 83, 84, 88, 93, 94, 95, 96, 98, 100, 101, 106, 108, 109, 116, 117, 119, 121, 125, 126, 128, 129, 131, 132, 134, 140, 141, 142, 144, 147, 153, 157, 158, 160, 163, 165, 166, 167, 168, 169, 170, 173, 174, 181, 183, 185, 187, 190, 191, 193, 194, 199, 201, 202, 203, 206, 207, 216, 217, 219, 225, 234, 235, 239, 243 and 245 based on results of binary integer linear programming [18] ensuring full network observability even in case of loss of

few PMUs. Maximum real and reactive power loadability of the system with optimally placed STATCOM were calculated for the system intact case and all the single line outage cases using flowchart shown in figure-4. In order to meet efficiency of STATCOM placement strategy, real and reactive power loadability were also calculated for the system in the absence of STATCOM, based on flowchart presented in figure-4 ignoring blocks corresponding to STATCOM. Real and reactive power loadability were also calculated for the system with and without STATCOM using continuation power flow (CPF) method. Real and reactive power loadability of the system with and without STATCOM has been shown in Table XI and XII respectively, for the system intact case and few critical contingency cases. It is observed from Table XI and Table XII that placement of STATCOM at optimal location (viz. bus number 174) results in significant enhancement in voltage stability margin. Figure-12 shows a comparison of the nose curves of critical bus 174 obtained using proposed approach with and without using STATCOM in the system for the line outage 156-158. Figure-13 also shows a comparison of the nose curves of critical bus 174 obtained using proposed approach with and without STATCOM in the system for the line outage 156-158. It is observed from figures-12 and 13 that STATCOM placed at bus-174 yields considerable enhancement in voltage stability margin.

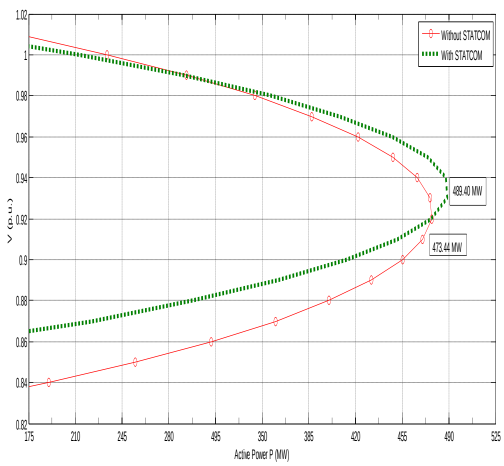

Figure 12: Comparison of *P-V* curves of critical bus 174 with STATCOM and without STATCOM for line outage 156-158 using PMU measurements

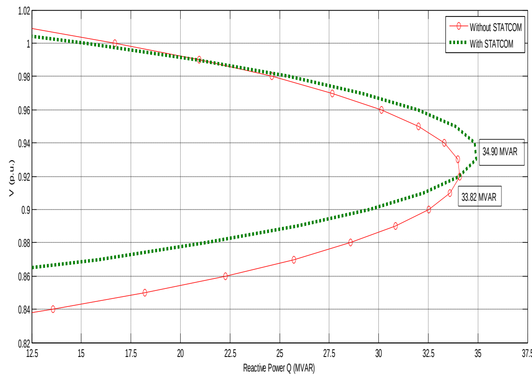

Figure 13: Comparison of *Q-V* curves of critical bus 174 with STATCOM and without STATCOM for line outage 156-158 using PMU measurements

TABLE XI
REALPOWERLOADABILITYOFTHESYSTEMWITHANDWITHOUT STATCOM

Critical Contingency	PMU Measurements		CPF Method	
	Without STATCOM P_D^{Max} (MW)	With STATCOM at bus-174 P_D^{Max} (MW)	Without STATCOM P_D^{Max} (MW)	With STATCOM at bus-174 P_D^{Max} (MW)
Intact	487.33	562.36	641.84	646.30
173-174	269.98	287.29	344.69	402.30
40-41	388.84	424.20	383.75	387.16
166-173	385.45	434.66	434.69	448.92
156-158	473.44	489.40	476.93	476.96
194-198	506.63	596.08	518.86	519.33

TABLE XII
REACTIVEPOWERLOADABILITYOFTHESYSTEMWITHANDWITHOUT STATCOM

Critical Contingency	PMU Measurements		CPF Method	
	Without STATCOM Q_D^{Max} (MVAR)	With STATCOM at bus-174 Q_D^{Max} (MVAR)	Without STATCOM Q_D^{Max} (MVAR)	With STATCOM at bus-174 Q_D^{Max} (MVAR)
Intact	38.80	44.77	51.11	51.47
173-174	21.50	22.88	27.45	32.04
40-41	30.96	33.78	30.56	30.83
166-173	30.69	34.61	34.61	35.74
156-158	33.82	34.90	34.07	37.08
63-70	19.51	21.68	19.33	21.50

V. CONCLUSIONS

Most of the research has concentrated on voltage stability monitoring and control of offline system. In this paper, real time monitoring and control of online system through reactive power injection by STATCOM has been proposed. Voltage stability margin has been monitored in real time framework based on voltage measurementobtained by PMUs at three consecutive operating points. STATCOM injects reactive power to the critical bus (the bus where it is placed) based on bus voltage magnitude differing from its reference value. Enhanced voltage stability margin as a result of reactive power injection is monitored at regular intervals using updated PMU measurements. Case studies performed on three test systems establish effectiveness of proposed approach of real time control of voltage stability margin through reactive power injection by STATCOM.

ACKNOWLEDGEMENTS

PankajSahu received his B.Tech degree in electrical engineering from Harcourt Butler Technological Institute, Kanpur, India in 2007 and M.Techdegreein electrical engineering from Motilal Nehru National Institute of Technology, Allahabad, India in 2010.He is currently persuing for PhD degreeat Indian Institute of Technology (BHU), Varanasi,India.
His research interestsinclude control system, instrumentation, voltage stability studies, wide area monitoring system and smart grid.

M. K. Verma received his B.Sc (Eng.) degree in electrical engineering from Regional Engineering College, Rourkela (presently National Institute of Technology, Rourkela), India in 1982, M.Sc (Eng.) degree in electrical engineering from Bihar Institute of Technology, Sindri, India in 1994 and PhD degree in electrical engineering from Indian Institute of Technology (IIT), Kanpur, India in 2005.

He is currently working as Professor in electrical engineering department at Indian Institute of Technology (BHU), Varanasi, India. His current research interests include voltage stability studies, application of FACTS controllers, power quality, wide area monitoring system and smart grid.

REFERENCES

[1] Byung Ha Lee and Kwang Y. Lee, "A Study on Voltage Collapse Mechanism in Electric Power Systems," *IEEE Trans. on Power Systems*,vol. 6, no. 3, August 1991.

[2] N. G. Hingorani and L. Gyugyi, "Understanding FACTS; Concepts and Technology of Flexible AC Transmission System," *IEEE Press*,NewYork, 2000.

[3] Mishra, P., Udupa, H. N., &Ghune, P.,"Calculation of Sensitive Node for IEEE–14 Bus System when Subjected to Various Changes in Load,"*In Proceedings of IRAJ International Conference,* 21st July 2013.

[4] Sanivarapu, Nagalakshmi, R. Kalaivani, and Dr SR Paranjothi. "Optimal Location of STATCOM to Improve Voltage Stability using PSO." *International journal of advanced engineering technology*, vol. 2, no. 4, 2011.

[5] Carson W. Taylor, Power System Voltage Stability, McGraw-Hill, Singapore, 1994.

[6] P.Kundur, Power System Stability and Control, McGraw-Hill, NY, 1994.

[7] N. Yorino, E. E. El-Araby, H. Sasaki and S. Harada, "A New Formulation for FACTS Allocation for Security Enhancement Against Voltage Collapse," *IEEE Trans. on Power Systems,* vol. 18, no. 1, pp. 3-10, February 2003.

[8] Park, Jong-Bae, Ki-Song Lee, Joong-Rin Shin, and Kwang Y. Lee. "A Particle Swarm Optimization for Economic Dispatch with Non-Smooth Cost Functions." *IEEE Transactions on Power systems,* vol. 20, no.1, pp. 34-42, February 2005.

[9] Kannan, S., S. Mary Raja Slochanal, and Narayana Prasad Padhy, "Application and Comparison of MetaheuristicTechniques to Generation Expansion Planning Problem." *IEEE Transactions on Power Systems*, vol. 20, no. 1, pp.466-475, February 2005.

[10] Huang, Chao-Ming, Chi-Jen Huang, and Ming-Li Wang. "A Particle Swarm Optimization to Identifying the ARMAX Model for Short-Term Load Forecasting." *IEEE Transactions on Power Systems*, vol. 20, no. 2 pp. 1126-1133, May 2005.

[11] J. Vishnu et al, "A Strategy for Optimal Loading Pattern of a Typical Power System – A Case Study," *International Conference on Advances in Green Energy (ICAGE),* pp. 112-117, 17-18 December 2014, Trivandrum, India.

[12] Bangjun Lei and ShuminFei, "IN H_∞Control for STATCOM to Improve Voltage Stability of Power System," Electronics Letter, vol. 53, no. 10, pp. 670-672, May 2017.

[13] Yan Xu et al, "Multi-Objective Dynamic VAR Planning Against Short-Term Voltage Instability Using a Decomposition-Based Evolutionary Algorithm," *IEEE Trans. on Power Systems,* vol. 29, no. 6, pp. 2813-2822, November 2014.

[14] KamelSayahi,AmeniKadri, RidhaKarwi and FaouziBacha, "Study and Implementation of a Static Compensator (STATCOM) Using

Direct Power Control Strategy," *IEEE 9th International Renewable Energy Congress (IREC)*, 20-22 March 2018, Hammamet, Tunisia.

[15] PankajSahu and M. K. Verma, "Online Voltage Stability Monitoring and Control in Smart Grid-A Survey," *IEEE UP Section Conference on Electrical, Computer and Electronics (UPCON)*, pp. 1-6, 4-6 December 2015, Allahabad, India.

[16] V. Ajjarapu, C. Christy, "The Continuation Power Flow: A Tool for Steady State Voltage Stability Analysis," *IEEE Trans. on Power Systems, vol.* 7, no. 1, pp. 416-423, February 1992.

[17] IEEE14-Bus System; [Available: http://www.ee.washington.edu/research/pstca/pf14/pg_tca14bus.htm]. [Accessed in April 2019].

[18] PankajSahu and M. K. Verma, "Optimal Placement of PMUs in Power System Network for Voltage Stability Estimation under Contingencies," 6th IEEE International Conference on Computer Applications In Electrical Engineering-Recent Advances (CERA),pp. 365-370, 5-7 October 2017, Roorkee, India.

[19] New England 39-Bus System; [Available: http://icseg.iti.illinois.edu/ieee-39-bus-system/]. [Accessed March/April 2019].

[20] North Region Power Grid (NRPG) 246-Bus System; 2013 [Available: http://www.iitk.ac.in/eeold/facilities/Research_labs/Power_System/NRPG-DATA.pdf]. [Accessed March 2019].